nature climate change

Analysis

https://doi.org/10.1038/s41558-023-01619-2

Increasing hypoxia on global coral reefs under ocean warming

Received: 23 April 2022

Accepted: 27 January 2023

Published online: 16 March 2023

Check for updates

Ariel K. Pezner[1], Travis A. Courtney[1,2], Hannah C. Barkley[3], Wen-Chen Chou[4,5], Hui-Chuan Chu[4], Samantha M. Clements[1], Tyler Cyronak[6], Michael D. DeGrandpre[7], Samuel A. H. Kekuewa[1], David I. Kline[8], Yi-Bei Liang[9], Todd R. Martz[1], Satoshi Mitarai[10], Heather N. Page[1,11], Max S. Rintoul[1], Jennifer E. Smith[1], Keryea Soong[9], Yuichiro Takeshita[12], Martin Tresguerres[1], Yi Wei[9,13], Kimberly K. Yates[14] & Andreas J. Andersson[1]

Ocean deoxygenation is predicted to threaten marine ecosystems globally. However, current and future oxygen concentrations and the occurrence of hypoxic events on coral reefs remain underexplored. Here, using autonomous sensor data to explore oxygen variability and hypoxia exposure at 32 representative reef sites, we reveal that hypoxia is already pervasive on many reefs. Eighty-four percent of reefs experienced weak to moderate (≤153 μmol O_2 kg^{-1} to ≤92 μmol O_2 kg^{-1}) hypoxia and 13% experienced severe (≤61 μmol O_2 kg^{-1}) hypoxia. Under different climate change scenarios based on four Shared Socioeconomic Pathways (SSPs), we show that projected ocean warming and deoxygenation will increase the duration, intensity and severity of hypoxia, with more than 94% and 31% of reefs experiencing weak to moderate and severe hypoxia, respectively, by 2100 under SSP5-8.5. This projected oxygen loss could have negative consequences for coral reef taxa due to the key role of oxygen in organism functioning and fitness.

Earth's global ocean has been steadily losing oxygen due to warming-induced decreases in oxygen solubility, accelerated respiration, increases in water column stratification and coastal eutrophication, commonly referred to as ocean deoxygenation[1–3]. Since the 1950s, the open ocean has lost more than 2% of its dissolved oxygen (DO), oxygen minimum zones have expanded and shoaled, and hundreds of coastal sites have reported severe hypoxic conditions (that is, aquatic oxygen levels below a given environmental threshold)[1–6]. These trends will continue in the future, as ocean surface oxygen concentrations are projected to decrease by an additional 3.2–3.7% by 2100, with oxygen loss expected to emerge across 59–80% of the ocean by 2050[4]. While trends of deoxygenation in the open ocean and the occurrence of temperate hypoxic and anoxic zones (defined as ≤2 mg O_2 l^{-1} and 0 mg O_2 l^{-1} (~61 μmol O_2 kg^{-1} and 0 μmol O_2 kg^{-1}) respectively[6]) are relatively well documented[1–3,6], there has been less focus on tropical coastal ecosystems, such as coral reefs[7–9], despite mounting evidence that modern hypoxic events can lead to mass mortality of coral reef taxa (for example, refs. [7–10]).

[1]Scripps Institution of Oceanography, University of California San Diego, La Jolla, CA, USA. [2]Department of Marine Sciences, University of Puerto Rico at Mayagüez, Mayagüez, Puerto Rico. [3]NOAA Pacific Islands Fisheries Science Center, Honolulu, HI, USA. [4]Institute of Marine Environment and Ecology, National Taiwan Ocean University, Keelung, Taiwan. [5]Center of Excellence for the Oceans, National Taiwan Ocean University, Keelung, Taiwan. [6]Institute for Coastal Plain Science, Georgia Southern University, Statesboro, GA, USA. [7]Department of Chemistry and Biochemistry, University of Montana, Missoula, MT, USA. [8]Smithsonian Tropical Research Institute, Ancón, Republic of Panama. [9]Department of Oceanography, National Sun Yat-sen University, Kaohsiung, Taiwan. [10]Marine Biophysics Unit, Okinawa Institute of Science and Technology, Okinawa, Japan. [11]Sea Education Association, Woods Hole, MA, USA. [12]Monterey Bay Aquarium Research Institute, Moss Landing, CA, USA. [13]Institute of Oceanography, National Taiwan University, Taipei, Taiwan. [14]United States Geological Survey, St. Petersburg Coastal and Marine Science Center, St Petersburg, FL, USA. e-mail: apezner@ucsd.edu

https://doi.org/10.1038/s41558-023-01619-2

Traditionally, coral reefs have been assumed to be well-oxygenated systems. However, autonomous, high-frequency DO measurements have been historically scarce in reef monitoring efforts[7–9]. As a result, there is a paucity of high-quality DO measurements from tropical coral reefs and a high likelihood that the occurrence of low oxygen events on tropical coral reefs across the globe has been severely underreported[7]. Acute, severe hypoxic events can be induced on tropical coral reefs through a variety of physical and biological mechanisms, such as warming, restricted water flow, increased biological oxygen demand, nutrient and organic matter loading, and an influx of oxygen-deficient water[7–10]. As global temperatures continue to increase and marine heatwaves become more frequent and severe[11], low oxygen conditions on coral reefs are likely to become more frequent as a result of changes in oxygen solubility and biological oxygen demand[12]. Given the essential role of oxygen in driving aerobic metabolism, hypoxia poses a serious threat to coral reef ecosystems and the humans that depend on them[3,8,13]. Thus, characterizing present-day oxygen concentrations on a variety of reefs across different spatiotemporal scales is imperative for defining 'normoxia' on tropical coral reefs, understanding the current extent of hypoxia exposure, and projecting future coral reef oxygen conditions under ocean warming and deoxygenation[8,9,13]. So far, a number of studies have expressed grave concerns about the potential consequences of declining available oxygen on coral reefs[7–9,13]. However, there are currently no synthesis studies characterizing the range of oxygen conditions experienced on global reefs today and what conditions reefs may experience in the future.

In this Analysis, we leveraged autonomous sensor data from 32 representative reef site deployments at 12 locations around the globe (Fig. 1a, Extended Data Fig. 1 and Supplementary Table 1) to quantify present-day oxygen conditions and hypoxia exposure at a diverse subset of reefs. We also modelled the effect of future warming scenarios on the oxygen solubility and the biological oxygen demand for each site and location to calculate decreases in oxygen availability (that is, deoxygenation) and hypoxic event frequency, duration, intensity and severity by 2100 (Methods). The observational data presented here include reef sites between 23° S and 32° N in the East and South China Sea; North Atlantic; West, Central and South Pacific; and Caribbean (Fig. 1a). Deployment lengths ranged from 3 to 309 days and occurred between 2013 and 2019 across seasons (see Supplementary Table 1 and Supplementary Methods for detailed site characterization and deployment information). Oxygen data were recorded at sites ranging from 0.7 m to 17.1 m in depth from a variety of coral reef habitat types (for example, reef fronts, terraces, reef flats, reef slopes, lagoons and patch reefs with different benthic communities; Supplementary Table 1).

Global variability in DO concentrations

We observed a large range of oxygen conditions among the different reef habitats, with diel oxygen variability, means and extremes differing between reef habitats at the same location, as well as between study locations in different regions (Fig. 1b,c, Extended Data Fig. 1 and Supplementary Table 2). The mean daily DO concentration across all sites was 173 ± 28 μmol O_2 kg^{-1} (mean ± 1 s.d.) or 88 ± 13% expressed as percent saturation, and the mean daily range was 81 ± 52 μmol O_2 kg^{-1} (42 ± 28% saturation). The mean daily minimum oxygen concentration was 136 ± 40 μmol O_2 kg^{-1} (69 ± 20% saturation), and the mean daily maximum was 217 ± 39 μmol O_2 kg^{-1} (111 ± 20% saturation), with large variations between reef locations (Figs. 1 and 2a, and Supplementary Table 2). The smallest mean daily range in oxygen (23 ± 4 μmol O_2 kg^{-1} and 12 ± 2%, respectively) was observed at the forereef in Tutuila, which was one of the deeper sites (15.2 m depth) and directly connected to the surrounding open ocean. In contrast, the largest mean daily range (258 ± 11 μmol O_2 kg^{-1} and 139 ± 5%, respectively) was observed at Taiping 1, which was a shallow (1 m) nearshore reef area dominated by seagrass and scattered coral colonies. At all locations, oxygen was typically lowest in the early morning and highest in the mid-afternoon as a result of nighttime respiration and daytime photosynthesis, respectively (Fig. 1b). A regression analysis of oxygen variability (mean daily range) as a function of mean depth (Supplementary Table 3) revealed a moderate, inverse nonlinear correlation (R^2 = 0.3; Extended Data Fig. 2a and Supplementary Table 4). No relationship was detected between oxygen variability and mean flow speed (R^2 = 0.002; Extended Data Fig. 2b and Supplementary Table 4). A positive, nonlinear correlation was observed between the mean daily oxygen minimum and mean flow speed (R^2 = 0.4; Extended Data Fig. 2c and Supplementary Table 4), whereas a weak nonlinear correlation was observed as a function of mean depth (R^2 = 0.1; Extended Data Fig. 2d and Supplementary Table 4). These results (Extended Data Fig. 2 and Supplementary Table 4) are in line with previous studies (for example, ref. [14]) linking shallower depths to greater variability in seawater chemistry on coral reefs due to a general increase in benthic biomass to water volume ratio. We observed no clear trend in oxygen variability based on the type of reef habitat (for example, reef fronts, terraces, reef flats, reef slopes, lagoons and patch reefs with different benthic communities; Supplementary Table 1).

Pervasive hypoxia under present-day conditions

While many aquatic studies use a threshold of ≤2 mg O_2 l^{-1} (~61 μmol O_2 kg^{-1} depending on seawater density) to define a hypoxic environment, DO thresholds vary as a function of taxa, exposure time, life stage, temperature and other factors[8,9,15–20]. Evidence from the few experiments conducted on tropical reef organisms suggests that lethal low oxygen thresholds can be as high as 4 mg O_2 l^{-1} (ref. [18]) and sublethal thresholds can be even higher for some species, especially under warming[17,19–21]. Thus, a threshold of 2 mg O_2 l^{-1} (61 μmol O_2 kg^{-1}) may not accurately capture the range of all the potential sublethal and lethal impacts of low oxygen for coral reef species. In our analyses, we employed four hypoxia thresholds: 'weak hypoxia' of ≤5 mg O_2 l^{-1} (153 μmol O_2 kg^{-1}), a conservative threshold that captures 90% of observed sublethal impacts in temperate benthic marine organisms[16], 'mild hypoxia' of ≤4 mg O_2 l^{-1} (122 μmol O_2 kg^{-1}), 'moderate hypoxia' of ≤3 mg O_2 l^{-1} (92 μmol O_2 kg^{-1}) and 'severe hypoxia' as the conventional ≤2 mg O_2 l^{-1} (61 μmol O_2 kg^{-1}) threshold (Methods).

On the basis of these thresholds, we found that many reef sites already experience oxygen stress. Nearly all reefs in our study (84%) experienced weak hypoxia, while 50%, 34% and 13% experienced mild, moderate and severe hypoxia, respectively, at some point during the data collection period (Figs. 1b,c and 2a–e). Across all sites, we identified 1,198 weak hypoxic events lasting 0.5 h to 64 h and 229 mild to moderate events lasting up to 18 h (Fig. 2b–e). Weak to moderate hypoxic events lasting less than 12 h were most common, whereas those lasting 12 h to 24 h or more than 24 h were comparatively rarer (Fig. 2b–e). Severe hypoxic events were less common (19 events observed at only 4 sites), with the longest event being 7.5 h in duration (Fig. 2b–e). The majority of hypoxic observations, regardless of threshold, occurred in the early morning between 02:00 and 07:00 due to net nighttime respiration (Fig. 3).

Hypoxia projections under warming and deoxygenation by 2100

To project future deoxygenation and resultant hypoxia exposure at each reef site, we employed location-specific projections of ocean warming by 2100 to calculate the cumulative effects of warming on oxygen solubility and biological oxygen demand. Warming projections were adopted from the Coupled Model Intercomparison Project Phase 6 (CMIP6) Shared Socioeconomic Pathways (SSPs) (Extended Data Fig. 3 and Supplementary Table 5)—SSP1-2.6 (+0.3 °C to +1.1 °C), SSP2-4.5 (+1.1 °C to +3.4 °C), SSP3-7.0 (+1.8 °C to +3.3 °C) and SSP5-8.5 (+2.8 °C to +4.1 °C) from the Community Earth System Model 2 Whole Atmosphere Community Climate Model (CESM2-WACCM; Methods)—and a severe, acute heatwave scenario of +6 °C (ref. [22]). The effect on oxygen

 https://doi.org/10.1038/s41558-023-01619-2

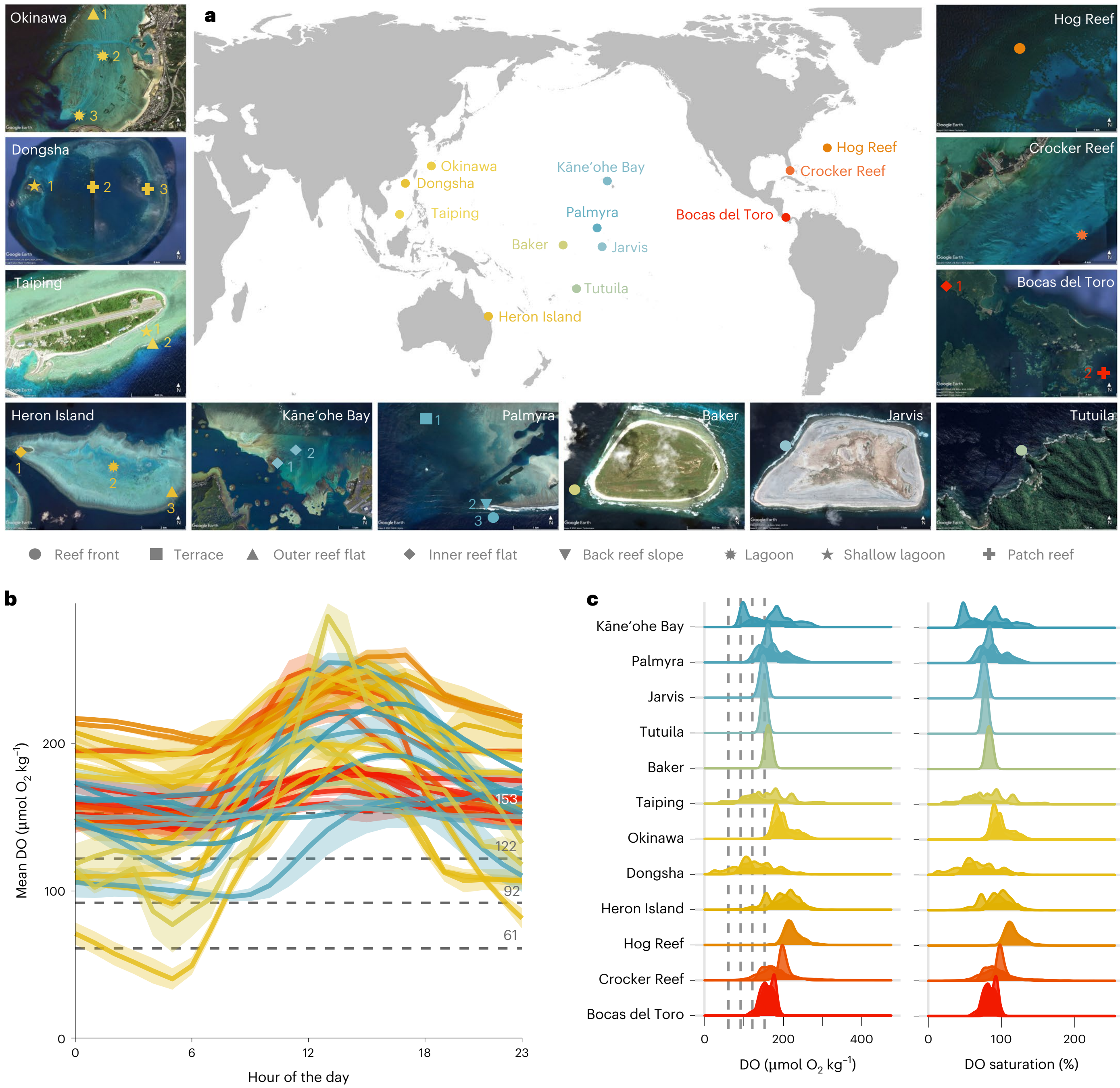

Fig. 1 | Oxygen sensor deployment sites and locations, hourly oxygen climatologies and oxygen distributions on global coral reefs. a, Map and satellite images of the study locations including specific instrument deployment sites (symbols) at each location. Reef type is indicated by the shape of the symbols according to the legend below the images. Some sites had instruments deployed at multiple depths or over multiple years and seasons (Supplementary Table 1). Map images and data: Google, Maxar Technologies, CNES/Airbus, SIO, NOAA, US Navy, NGA and GEBCO. **b**, Mean ± shaded lower and upper 95% confidence interval of the hourly climatology of DO concentrations for all sites (*n* varies by site; Supplementary Table 2). The grey dashed lines indicate the four hypoxia thresholds: 153 μmol O_2 kg^{-1}, 122 μmol O_2 kg^{-1}, 92 μmol O_2 kg^{-1} and 61 μmol O_2 kg^{-1}. **c**, Ridgeline distributions of DO concentration and percent saturation grouped by location. Vertical grey dashed lines indicate four hypoxia concentration thresholds as in **b**. In all panels, the colour scheme follows the location colours used in **a**.

solubility was calculated based on thermodynamic principles, and the effect on biological oxygen demand was approximated from night-time respiration signals and a temperature coefficient (Q_{10}) (Methods and Extended Data Fig. 4). These calculations inherently account for site-specific properties that influence seawater oxygen concentrations, such as community composition, flow rates and residence time, but do not account for potential future changes to these properties.

To verify our approach, we also employed a simple box model to assess the validity of our calculations under a range of temperature and residence time scenarios (Methods and Extended Data Fig. 5).

Our results reveal that under the SSP1-2.6 scenario, the number of reef sites assessed in this study experiencing weak hypoxia by 2100 would be similar to present-day observations (84%), increasing to 94% under SSP5-8.5 and 97% during a 6 °C heatwave event (Fig. 2a and

 https://doi.org/10.1038/s41558-023-01619-2

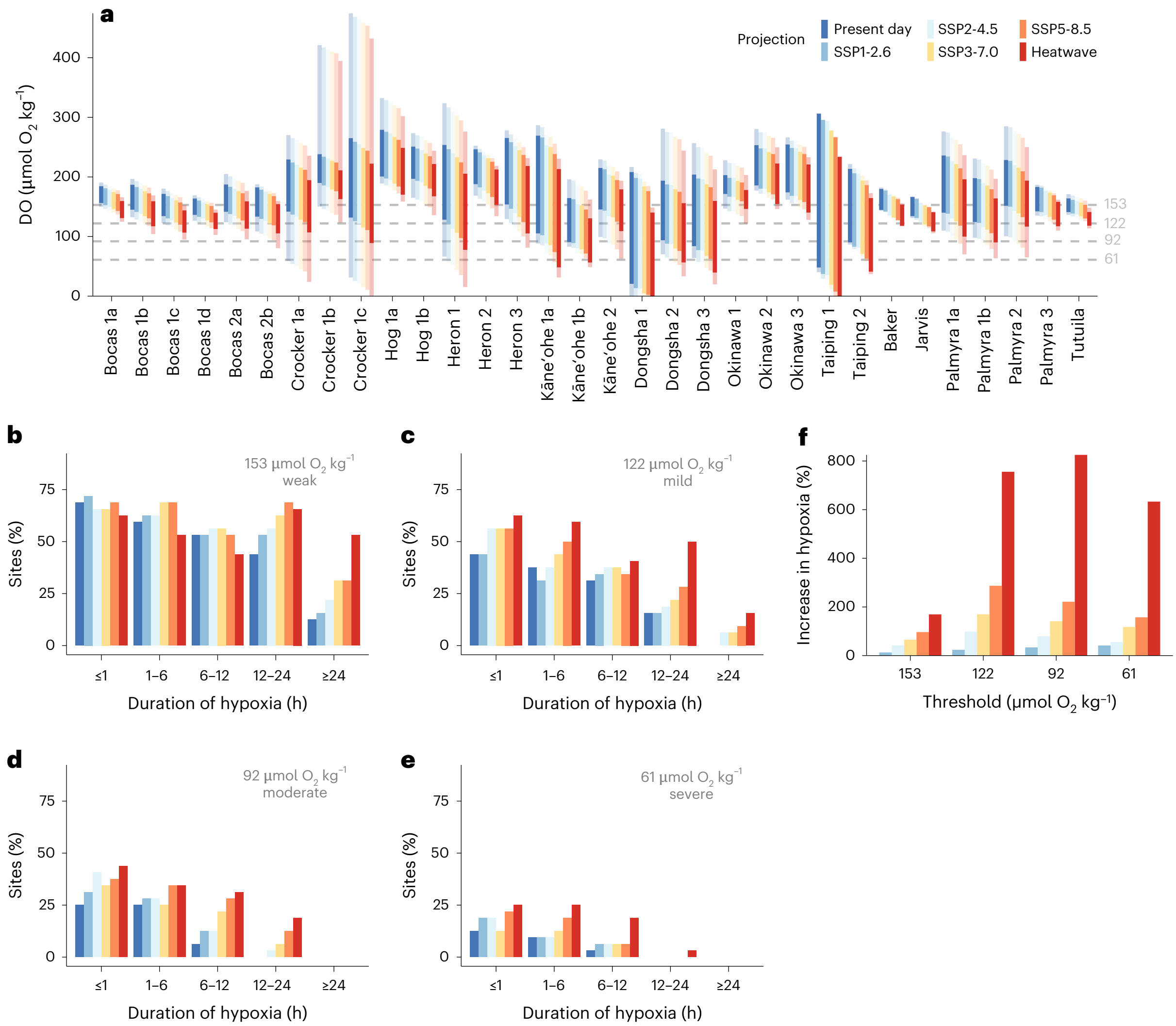

Fig. 2 | Shifts in DO concentration, hypoxic event duration and occurrence of hypoxia exposure under warming on global coral reef sites. **a**, DO (μmol O_2 kg^{-1}) for the present day and under five different warming projections (including four SSPs and a heatwave scenario; blue to red). Vertical dark shaded bars represent the mean daily range of DO for each reef site (*n* varies by site; Supplementary Table 2 and Table 5). The lower and upper bounds of the vertical light shaded bars represent the lowest daily minimum oxygen and highest daily maximum oxygen concentration, respectively (*n* varies by site; Supplementary Table 2). The grey dashed lines indicate the hypoxia thresholds: 153 μmol O_2 kg^{-1} (weak), 122 μmol O_2 kg^{-1} (mild), 92 μmol O_2 kg^{-1} (moderate) and 61 μmol O_2 kg^{-1} (severe). Within each location, different instrument deployment sites are represented by numbers (for example, Dongsha 1 and Dongsha 2) or a combination of letters and numbers where letters represent either different depths at the same site (for example, Bocas 1a and 1b) or different deployments at the same site over time (for example, Crocker 1a, 1b and 1c) (see Supplementary Table 1 for specific site information). **b**–**e**, Percent of sites ($n = 32$) that experience hypoxic events of different durations (*x* axis, hours) for the present day and for each warming projection (blue to red) and hypoxia threshold: 153 μmol O_2 kg^{-1} (**b**), 122 μmol O_2 kg^{-1} (**c**), 92 μmol O_2 kg^{-1} (**d**) and 61 μmol O_2 kg^{-1} (**e**). **f**, Percent increase in the total number of observations below each hypoxia threshold (153 μmol O_2 kg^{-1}, 122 μmol O_2 kg^{-1}, 92 μmol O_2 kg^{-1} and 61 μmol O_2 kg^{-1}) across all sites for each warming projection relative to the present day.

Supplementary Table 6). The number of sites experiencing mild and moderate hypoxia would increase from 59% and 34%, respectively, under SSP1-2.6, to 72% and 44% of sites under the SSP5-8.5 scenario (Fig. 2a and Supplementary Table 6) and 75% and 53% during a 6 °C heatwave. Further, under the SSP1-2.6 scenario, 19% of sites would experience severe hypoxia by the year 2100, increasing to 31% under the SSP5-8.5 scenario and 34% during a 6 °C heatwave event (Fig. 2a and Supplementary Table 6).

The percent of sites experiencing longer durations of hypoxia will also increase under warming across all the thresholds considered (Fig. 2b–e and Supplementary Table 7). More than 28% of sites would experience mild hypoxic events lasting between 12 h and 24 h under the SSP5-8.5 scenario, increasing to 50% of sites under a 6 °C heatwave, compared with 16% for the present day (Fig. 2c and Supplementary Table 7). Similarly, the percent of sites experiencing severe hypoxic events of 6 h to 12 h in duration would increase from just 3% for the present day to 6.3% under SSP5-8.5 and 19% under a 6 °C heatwave (Fig. 2e and Supplementary Table 7).

Overall, by 2100, the total number of hypoxic observations will increase under all warming scenarios, ranging from an increase of 13% to 42% under SSP1-2.6 and 97% to 287% under SSP5-8.5 (Fig. 2f and Extended Data Fig. 6) relative to the present day. As a result, the frequency, duration, intensity (that is, the difference between a threshold and the measured concentration[23]) and severity (average intensity multiplied by duration[23]) of hypoxic events crossing each threshold will also increase (Methods, Fig. 2, Extended Data Figs. 6–8 and Supplementary Tables 6 and 7). These projections suggest a shift from more acute to more chronic hypoxia exposure under increasing warming, the

https://doi.org/10.1038/s41558-023-01619-2

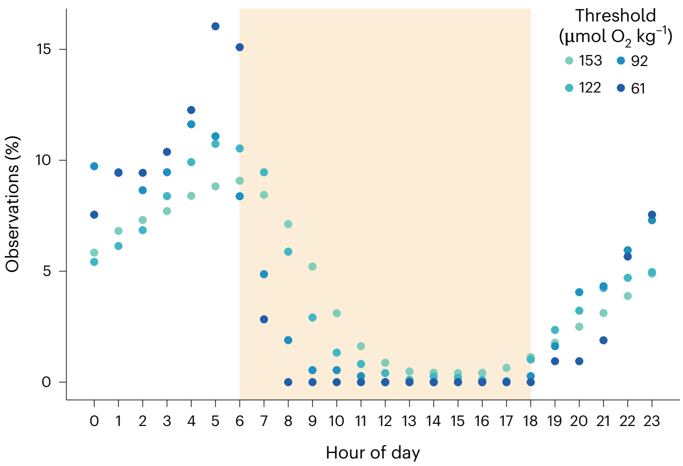

Fig. 3 | Timing of present-day hypoxic observations across global coral reef sites. Percent of recorded DO observations below each hypoxia threshold (153 μmol O_2 kg^{-1}, 122 μmol O_2 kg^{-1}, 92 μmol O_2 kg^{-1} and 61 μmol O_2 kg^{-1}; light to dark blue) occurring at each hour of the day for all global coral reef sites and deployments. Daylight hours are denoted by the orange shaded box (local time).

magnitude of which will depend on future atmospheric CO_2 concentrations and the relevant thresholds of hypoxia tolerance for reef taxa (Fig. 2, Extended Data Figs. 6–8 and Supplementary Tables 6 and 7).

Implications of increasing hypoxia

A better understanding of what changing oxygen dynamics on coral reefs means for corals and reef ecosystems is needed. Field data from severe hypoxic events on coral reefs show extremely variable responses of different coral genera[8], revealing both sensitive (for example, *Acropora* and *Pocillopora* spp.) and tolerant (for example, *Porites* spp.) groups[7,24–26]. Similarly, data from the relatively few laboratory low-oxygen experiments we could find in the literature for tropical corals reveal a wide range of species-specific tolerances to low oxygen intensity and duration under both constant and nightly low oxygen exposure regimes (for a literature review, see Supplementary Table 8). For example, under constant exposure to severe hypoxia of 1 mg O_2 l^{-1} (~31 μmol O_2 kg^{-1}), *Acropora cervicornis* experienced tissue loss, bleaching and mortality after 2 days, whereas *Orbicella faveolata* survived more than 11 days under the same conditions[19]. In another study, *Agaricia lamarcki* survived 7 days of exposure to hypoxic conditions of 0.5 mg O_2 l^{-1} (~15 μmol O_2 kg^{-1}), whereas all *Stephanocoenia intersepta* colonies experienced complete mortality[7], suggesting some species or populations may be particularly resilient (or susceptible) to low oxygen stress. On the basis of the results of the present study, none of our reef sites are projected to experience multi-day severe hypoxia under the warming scenarios used in our analyses. However, these conditions may still occur on these reefs in the future. Data from field observations show that additional drivers, such as reduced winds, slow flow, stratification, reduced mixing, and other unique meteorological or oceanographic conditions, can and will interact to lead to acute, severe hypoxic events of comparable intensity and duration on reefs[7,8,10,24–27], which will be further exacerbated by warming[28].

Importantly, exposure to nighttime (<12 h) low oxygen conditions alone with reoxygenation during daytime has been shown to cause both sublethal and lethal impacts in tropical corals under a range of oxygen concentrations (Supplementary Table 8). *Acropora yongei* exposed to nightly mild to moderate hypoxia of 2–4 mg O_2 l^{-1} (61–122 μmol O_2 kg^{-1}) experienced partial to full mortality and substantial tissue loss after just 3 days[18]. Similarly, the majority of *Montipora capitata* corals exposed to nightly anoxia (0 mg O_2 l^{-1}) experienced bleaching after just 2 days and full mortality within 5 days[29]. At the sublethal level, bleaching[29,30], tissue loss[18,29], reductions in calcification rates[31–33], DNA damage[34], changes in gene expression[30,35], shifts in metabolism[29] and reductions in photosynthetic capacity[18] have all been observed in a variety of coral species exposed to only nighttime hypoxia (<12 h) of varying intensity (Supplementary Table 8), highlighting the potential consequences of even short-term exposure to low oxygen conditions. For the reef habitats surveyed in the present study, we project an increase in the number of sites experiencing hypoxic events lasting between 12 h and 24 h under increasing warming across all thresholds (Fig. 2b–e and Supplementary Table 7). For example, the percent of sites experiencing mild hypoxic events (≤4 mg O_2 l^{-1} or 122 μmol O_2 kg^{-1}) lasting 12–24 h would nearly double under an SSP5-8.5 warming scenario (increasing from 16% to 28%) and more than triple under an acute 6 °C heatwave event (50% of sites), posing a potential threat to the more sensitive corals at these sites (Fig. 2c and Supplementary Table 7). While reef habitats tend to experience low oxygen conditions at night regularly under present-day conditions (Fig. 3), increased intensity and/or duration of nighttime hypoxic exposure may have pronounced sublethal to lethal effects on corals, as accumulated oxygen produced through light-driven photosynthesis in the daytime may not be enough to effectively buffer against lower nighttime oxygen conditions[31–33].

Physiologically, some coral species may be able to cope with varying degrees of hypoxia (here, insufficient supply of O_2 to tissues to maintain normal functioning) by increasing anaerobic respiration[29] and engaging transcriptional hypoxia response systems[30,36] (Supplementary Table 8). However, these strategies may not be equally effective for all corals or sustainable under repeated stress or longer hypoxic events. Studies of coral larvae and recruits demonstrate that hypoxic conditions can impair coral settlement[37], reduce survivorship of coral recruits[38] and hinder the expression of key genes associated with early development regulation[35], further limiting ecosystem recovery under repeated or long-term hypoxic conditions.

Low oxygen tolerance also varies between reef-associated organisms by orders of magnitude, with some thresholds well above the generalized environmental hypoxia threshold of 2 mg O_2 l^{-1} for aquatic organisms. A 2008 meta-analysis of temperate species found bivalves and gastropods were the most tolerant to low oxygen, whereas crustaceans and fishes were the most sensitive in terms of mortality[16]. Median lethal time also varied substantially both between and within taxonomic groups, ranging from 23 min for a species of flounder to 32 weeks for a species of bivalve[16]. Aside from direct mortality, organisms experiencing intratissue hypoxia can experience changes in behaviour, feeding, respiration, reproduction and/or general performance, which can scale up to impair ecosystem function through loss or migration of key species[6,8]. It will also be important to understand the tolerance of photosynthetic organisms to low oxygen, as a reduction in photosynthetic activity during the day will have implications for the mean and extreme oxygen conditions on a reef[8].

Notably, oxygen loss and hypoxic events are not occurring in isolation from other stressors. Oxygen and temperature are tightly linked in terms of organism metabolism and together may severely limit species performance and restrict the availability of habitats that are metabolically viable[17,28,39,40]. For tropical corals, there is evidence that the ability to effectively respond to low oxygen conditions and overcome a metabolic crisis is a key factor in determining bleaching tolerance versus susceptibility[30,41]. In addition, low oxygen conditions typically co-occur with acidification, as increased respiration decreases both pH and DO concentrations[28]. The combination of low oxygen and acidification stress has been shown to be mainly additive, with negative impacts across a wide range of taxa[42]. Coastal eutrophication, which drives increased respiration, therefore has the capacity to intensify local hypoxia and acidification, suggesting a reduction of nutrient and organic matter inputs may improve projected conditions at local scales under ongoing global change[43,44].

Here we provide a comprehensive synthesis of oxygen concentrations and variability as well as hypoxia frequency, intensity, severity and duration on tropical coral reefs. Our findings suggest that hypoxia is already pervasive in coral reef habitats around the world and will become more frequent and severe as ocean temperatures increase. While these projections are specific to the reefs and locations included in this study, and our calculations are limited by the available environmental and physical data for each reef, the observations presented here provide broad representation of different reef systems and environments found around the world. Continued and additional high-frequency oxygen data measurements on coral reefs over different seasons and longer timescales will be imperative for establishing baseline conditions, tracking potential hypoxic events, expanding the applicability of these predictions and characterizing impacts on reef communities in the future. Further, depositing data in public repositories can help to ensure data transparency and encourage data sharing (for example, GO2DAT[45], or other commonly used and open-access databases). At the same time, field and laboratory experiments must aim to further refine accurate and realistic thresholds and durations of exposure to low oxygen for different coral reef organisms to better predict future impacts on reef ecology, health and function.

Online content

Any methods, additional references, Nature Portfolio reporting summaries, source data, extended data, supplementary information, acknowledgements, peer review information; details of author contributions and competing interests; and statements of data and code availability are available at https://doi.org/10.1038/s41558-023-01619-2.

References

1. Stramma, L., Johnson, G. C., Sprintall, J. & Mohrholz, V. Expanding oxygen-minimum zones in the tropical oceans. *Science* **320**, 655–658 (2008).
2. Keeling, R. F., Körtzinger, A. & Gruber, N. Ocean deoxygenation in a warming world. *Ann. Rev. Mar. Sci.* **2**, 199–229 (2010).
3. Breitburg, D. et al. Declining oxygen in the global ocean and coastal waters. *Science* **359**, eaam7240 (2018).
4. Bopp, L. et al. Multiple stressors of ocean ecosystems in the 21st century: projections with CMIP5 models. *Biogeosciences* **10**, 6225–6245 (2013).
5. Kwiatkowski, L. et al. Twenty-first century ocean warming, acidification, deoxygenation, and upper-ocean nutrient and primary production decline from CMIP6 model projections. *Biogeosciences* **17**, 3439–3470 (2020).
6. Diaz, R. J. & Rosenberg, R. Marine benthic hypoxia: a review of its ecological effects and the behavioural responses of benthic macrofauna. *Oceanogr. Mar. Biol.* **33**, 245–303 (1995).
7. Altieri, A. H. et al. Tropical dead zones and mass mortalities on coral reefs. *Proc. Natl Acad. Sci. USA* **114**, 3660–3665 (2017).
8. Nelson, H. R. & Altieri, A. H. Oxygen: the universal currency on coral reefs. *Coral Reefs* **38**, 177–198 (2019).
9. Hughes, D. J. et al. Coral reef survival under accelerating ocean deoxygenation. *Nat. Clim. Change* **10**, 296–307 (2020).
10. Kealoha, A. K. et al. Localized hypoxia may have caused coral reef mortality at the Flower Garden Banks. *Coral Reefs* **39**, 119–132 (2020).
11. Frölicher, T. L., Fischer, E. M. & Gruber, N. Marine heatwaves under global warming. *Nature* **560**, 360–364 (2018).
12. Vaquer-Sunyer, R., Duarte, C. M., Jordà, G. & Ruiz-Halpern, S. Temperature dependence of oxygen dynamics and community metabolism in a shallow Mediterranean macroalgal meadow (*Caulerpa prolifera*). *Estuaries Coast.* **35**, 1182–1192 (2012).
13. Sutherland, W. J. et al. A 2021 horizon scan of emerging global biological conservation issues. *Trends Ecol. Evol.* **36**, 87–97 (2021).
14. Cyronak, T. et al. Diel temperature and pH variability scale with depth across diverse coral reef habitats. *Limnol. Oceanogr. Lett.* **5**, 193–203 (2020).
15. Gray, J. S., Wu, R. S. S. & Or, Y. Y. Effects of hypoxia and organic enrichment on the coastal marine environment. *Mar. Ecol. Prog. Ser.* **238**, 249–279 (2002).
16. Vaquer-Sunyer, R. & Duarte, C. M. Thresholds of hypoxia for marine biodiversity. *Proc. Natl Acad. Sci. USA* **105**, 15452–15457 (2008).
17. Vaquer-Sunyer, R. & Duarte, C. M. Temperature effects on oxygen thresholds for hypoxia in marine benthic organisms. *Glob. Change Biol.* **17**, 1788–1797 (2011).
18. Haas, A. F., Smith, J. E., Thompson, M. & Deheyn, D. D. Effects of reduced dissolved oxygen concentrations on physiology and fluorescence of hermatypic corals and benthic algae. *PeerJ* **2**, e235 (2014).
19. Johnson, M. D., Swaminathan, S. D., Nixon, E. N., Paul, V. J. & Altieri, A. H. Differential susceptibility of reef-building corals to deoxygenation reveals remarkable hypoxia tolerance. *Sci. Rep.* **11**, 23168 (2021).
20. Gravinese, P. M., Douwes, A., Eaton, K. R. & Muller, E. M. Ephemeral hypoxia reduces oxygen consumption in the Caribbean coral *Orbicella faveolata*. *Coral Reefs* **41**, 13–18 (2021).
21. Nilsson, G. E., Östlund-Nilsson, S. & Munday, P. L. Effects of elevated temperature on coral reef fishes: loss of hypoxia tolerance and inability to acclimate. *Comp. Biochem. Physiol.* **156**, 389–393 (2010).
22. DeCarlo, T. M. et al. Mass coral mortality under local amplification of 2 °C ocean warming. *Sci. Rep.* **7**, 44586 (2017).
23. Hauri, C., Gruber, N., McDonnell, A. M. P. & Vogt, M. The intensity, duration, and severity of low aragonite saturation state events on the California continental shelf. *Geophys. Res. Lett.* **40**, 3424–3428 (2013).
24. Guzmán, H. M., Cortés, J., Glynn, P. W. & Richmond, R. H. Coral mortality associated with dinoflagellate blooms in the Eastern Pacific (Costa Rica and Panama). *Mar. Ecol. Prog. Ser.* **60**, 299–303 (1990).
25. Raj, K. D. et al. Low oxygen levels caused by Noctiluca scintillans bloom kills corals in Gulf of Mannar, India. *Sci. Rep.* **10**, 22133 (2020).
26. Johnson, M. D. et al. Rapid ecosystem-scale consequences of acute deoxygenation on a Caribbean coral reef. *Nat. Commun.* **12**, 4522 (2021).
27. Andréfouët, S., Dutheil, C., Menkes, C. E., Bador, M. & Lengaigne, M. Mass mortality events in atoll lagoons: environmental control and increased future vulnerability. *Glob. Change Biol.* **21**, 195–205 (2015).
28. Altieri, A. H. & Gedan, K. B. Climate change and dead zones. *Glob. Change Biol.* **21**, 1395–1406 (2015).
29. Murphy, J. W. A. & Richmond, R. H. Changes to coral health and metabolic activity under oxygen deprivation. *PeerJ* **4**, e1956 (2016).
30. Alderdice, R. et al. Divergent expression of hypoxia response systems under deoxygenation in reef-forming corals aligns with bleaching susceptibility. *Glob. Change Biol.* **27**, 312–326 (2021).
31. Al-Horani, F. A., Tambutté, É. & Allemand, D. Dark calcification and the daily rhythm of calcification in the scleractinian coral, *Galaxea fascicularis*. *Coral Reefs* **26**, 531–538 (2007).
32. Wijgerde, T., Jurriaans, S., Hoofd, M., Verreth, J. A. J. & Osinga, R. Oxygen and heterotrophy affect calcification of the scleractinian coral *Galaxea fascicularis*. *PLoS ONE* **7**, e52702 (2012).
33. Wijgerde, T., Silva, C. I. F., Scherders, V., van Bleijswijk, J. & Osinga, R. Coral calcification under daily oxygen saturation and pH dynamics reveals the important role of oxygen. *Biol. Open* **3**, 489–493 (2014).
34. Deleja, M. et al. Effects of hypoxia on coral photobiology and oxidative stress. *Biology* **11**, 1068 (2022).

35. Alderdice, R. et al. Hypoxia as a physiological cue and pathological stress for coral larvae. *Mol. Ecol.* **31**, 571–587 (2022).
36. Alderdice, R. et al. Disparate inventories of hypoxia gene sets across corals align with inferred environmental resilience. *Front. Mar. Sci.* **9**, 834332 (2022).
37. Jorissen, H. & Nugues, M. M. Coral larvae avoid substratum exploration and settlement in low-oxygen environments. *Coral Reefs* **9**, 31–39 (2021).
38. Villanueva, R. D., Yap, H. T. & Montaño, M. N. E. Survivorship of coral juveniles in a fish farm environment. *Mar. Pollut. Bull.* **10**, 580–589 (2005).
39. Pörtner, H.-O., Bock, C. & Mark, F. C. Oxygen- and capacity-limited thermal tolerance: Bridging ecology and physiology. *J. Exp. Biol.* **220**, 2685–2696 (2017).
40. Deutsch, C., Ferrel, A., Seibel, B., Pörtner, H.-O. & Huey, R. B. Climate change tightens a metabolic constraint on marine habitats. *Science* **348**, 1132–1135 (2015).
41. Alderdice, R. et al. Deoxygenation lowers the thermal threshold of coral bleaching. *Sci. Rep.* **12**, 18273 (2022).
42. Steckbauer, A., Klein, S. G. & Duarte, C. M. Additive impacts of deoxygenation and acidification threaten marine biota. *Glob. Change Biol.* **26**, 5602–5612 (2020).
43. Cai, W. J. et al. Acidification of subsurface coastal waters enhanced by eutrophication. *Nat. Geosci.* **4**, 766–770 (2011).
44. D'Angelo, C. & Wiedenmann, J. Impacts of nutrient enrichment on coral reefs: new perspectives and implications for coastal management and reef survival. *Curr. Opin. Environ. Sustain.* **7**, 82–93 (2014).
45. Grégoire, M. et al. A global ocean oxygen database and atlas for assessing and predicting deoxygenation and ocean health in the open and coastal ocean. *Front. Mar. Sci.* **8**, 724913 (2021).

https://doi.org/10.1038/s41558-023-01619-2

Methods

Sensor and deployment information

The majority of DO data presented in the current study (25 of 32 sites) were recorded by SeapHOx or Sea-Bird Scientific conductivity, temperature and depth (CTD) sensor packages with Aanderaa oxygen optodes (Supplementary Table 1). The remaining oxygen datasets were recorded by Idronaut CTD and oxygen sensor packages (Dongsha 1 and Dongsha 2), Sea-Bird SBE19 plus CTD and SBE 43 oxygen sensor packages (Baker, Jarvis, Palmyra 3 and Tutuila), or Sea-Bird Scientific CTD and PME miniDOT sensor packages (Taiping 1). Detailed site and deployment information can be found in Supplementary Methods. For each location, different instrument deployment sites are represented by numbers (for example, Dongsha 1 and Dongsha 2) or a combination of letters and numbers where letters represent either different depths at the same site (for example, Bocas 1a, 1b, 1c and 1d) or different deployments at the same site over time (for example, Crocker 1a, 1b and 1c).

Calibrations and conversions of datasets

All sensors were calibrated by the manufacturer or according to the manufacturer's instructions by the user as noted in previous publications[46–53]. If applicable, salinity corrections were implemented according to the manufacturer's specifications, and analogue measurements were converted from voltages to concentrations. Data were assessed for quality and erroneous data points (defined as missing values or values that exceeded the measurement range of the instrument), which were flagged and excluded from any subsequent analyses. Deployment data were restricted to measurements in seawater based on salinity values to exclude extraneous data points collected during instrument transport, initial deployment or recovery (exposure to air). Density calculations using the Gibbs SeaWater Toolbox functions[54] in RStudio[55] were used to convert all oxygen concentration units to μmol O_2 kg^{-1}. See Supplementary Methods (and Supplementary Table 9) for an assessment and discussion on the potential errors and uncertainty of the oxygen measurements. All data[56] and relevant code[57] files are available for download online and may be used with proper attribution.

Literature review of tropical coral low oxygen experiments

To place our results into a context of reported tropical coral responses to low oxygen conditions, we conducted a literature review of published, peer-reviewed studies that tested the effects of low oxygen conditions on tropical corals (Supplementary Table 8). The review was conducted using references cited in previous review papers[8,9] as well as searches on Google Scholar of 'coral hypoxia experiment', 'coral oxygen experiment' and 'coral anoxia experiment' and references of papers found via these searches. Experiments testing oxygen alone or in combination with other stressors were included. In total, 16 studies were identified testing 19 different species of tropical corals (Supplementary Table 8).

Calculations of daily statistics

The mean and absolute daily minimum and maximum (Fig. 2a and Supplementary Table 2) as well as the mean daily range (Supplementary Table 2) were calculated for each site. These calculations excluded partial days of data (that is, the first and last days of the deployment were excluded to avoid bias) to ensure means and extremes were calculated over full 24 h cycles.

Depth, flow speed and reef type analyses

To test the influence of depth, flow speed and reef type on oxygen variability, we performed regression analyses to assess the relationship between (1) oxygen variability, depth and reef type; (2) oxygen variability, flow speed and reef type; (3) oxygen minimum, depth and reef type; and (4) oxygen minimum, flow speed and reef type. Oxygen variability was defined as the mean daily range in DO for each site, and oxygen minimum was defined as the mean daily minimum DO for each site (both in μmol O_2 kg^{-1}). Depth used was either the depth provided by the data owners and reported in the relevant studies (Supplementary Table 1) or as the mean ± 1 s.d. as recorded by current meters deployed alongside the oxygen sensors at select sites. Mean flow speed was calculated as the mean, depth-integrated flow speed from current meters that were co-deployed with a subset of the oxygen sensors used in this study. The analyses using depth and oxygen variability or oxygen minimum were performed for all sites, excluding Hog 1a, as this sensor was not deployed on the benthos. The analyses using flow speed were only performed for a subset of sites where flow meters were deployed at the same time and in the same location as the oxygen sensor (Supplementary Table 3). Reef type was defined for each site using a published guide of reef cover classifications ([58]; Supplementary Table 1). Regression coefficients were determined using the MATLAB Curve Fitting Toolbox (version 3.8) using a Power fit type (as in ref. [14]; Supplementary Table 4).

Calculations of intensity, duration and severity

The intensity (I), duration (D) and severity (S) of hypoxic observations and events were calculated by modifying a methodology applied to seawater aragonite saturation states by ref. [23] according to equations (1)–(3) below. Before calculations, datasets that were not at a 30 min sampling frequency were either subsampled (Dongsha 1, Dongsha 2, Hog 1a, Hog 1b, Dongsha 3, Okinawa 2, Okinawa 3, Taiping 1, Taiping 2, Tutuila, Baker, Jarvis and Palmyra 3) or interpolated (Crocker 1a, 1b and 1c and Palmyra 1b) to a 30 min sampling frequency to standardize comparisons across datasets. Linear interpolations were performed using the approx() function in RStudio[55].

For individual hypoxic observations, the intensity (I_{obs}, μmol O_2 kg^{-1}) was calculated as the difference between the observed oxygen concentration (DO_{obs}, μmol O_2 kg^{-1}) and the threshold of hypoxia (T, μmol O_2 kg^{-1}):

$$I_{obs} = T - DO_{obs} \tag{1}$$

For hypoxic events, consecutive observations below a given oxygen threshold were identified using the rleid() function of the data.table package[59] in RStudio[55,57]. Intensity of the event (I_{event}, μmol O_2 kg^{-1}) was calculated as the difference between the threshold (T) and the mean oxygen concentration during the event ($\overline{DO}_{event}$):

$$I_{event} = T - \overline{DO}_{event} \tag{2}$$

Severity of the event (S, μmol O_2 kg^{-1} h) was calculated as the product of the event intensity (I_{event}) and duration (D, h)[23]:

$$S = I_{event} \times D \tag{3}$$

For these calculations, we used four hypoxia thresholds: 153 μmol O_2 kg^{-1} (~5 mg O_2 l^{-1}), 122 μmol O_2 kg^{-1} (~4 mg O_2 l^{-1}), 92 μmol O_2 kg^{-1} (~3 mg O_2 l^{-1}) and 61 μmol O_2 kg^{-1} (~2 mg O_2 l^{-1}). While many aquatic studies use the threshold of ≤2 mg O_2 l^{-1} (~61 μmol O_2 kg^{-1}) to define environmental DO levels as hypoxic, it has been shown that this threshold, originally identified as the level at which great reductions in benthic macrofauna would be observed in northern European fjords[60], is inadequate as a threshold for all marine species[15,16,61]. We provide the three additional thresholds to better capture a range of organism sensitivities to both lethal and sublethal impacts. On the basis of Vaquer–Sunyer and Duarte[16], we chose a 'weak' hypoxia threshold of 153 μmol O_2 kg^{-1} (~5 mg O_2 l^{-1}) as the upper bound of our thresholds, as it is the oxygen concentration that captured 90% of sublethal impacts in temperate benthic marine organisms. We then added thresholds at regular intervals between the severe and weak thresholds, with a 'mild' hypoxia threshold of 122 μmol O_2 kg^{-1} (~4 mg O_2 l^{-1}, an upper bound of lethal oxygen levels determined for the tropical coral *Acropora yongei*[18]) and a 'moderate' hypoxia threshold of 92 μmol O_2 kg^{-1} (~3 mg O_2 l^{-1}). The terminology of 'deoxygenation' was not used to refer to these thresholds, as 'ocean deoxygenation' has been previously defined as "the global process of declining O_2 concentrations projected to occur over an extended period, decades or longer, caused predominantly by processes resulting from climate change"[62], and thus is a process occurring on a much greater time and space scale than the individual reef habitats we surveyed here. Calculations of intensity (for events and observations), duration of events and severity of events were performed for each threshold (Fig. 2b–f and Extended Data Figs. 6–8).

Temperature projection data

We extracted predicted sea surface temperature (SST) rise values for each location (Extended Data Fig. 3) from the CMIP6 ensemble member Community Earth System Model 2 Whole Atmosphere Community Climate Model[63,64] (CESM2-WACCM). The model was run by the National Center for Atmospheric Research in 2018, with a 0.9° × 1.25° finite volume grid atmosphere with 70 levels coupled with a 320 × 384 longitude/latitude ocean with 60 levels[63,64]. The model used the historical, SSP1-2.6, SSP2-4.5, SSP3-7.0 and SSP5-8.5 simulations[63,64]. Monthly SST data from the closest grid cell to each location's latitude and longitude were averaged and compared between the present day (mean of the 2015–2020 annual SST) and the end of century (mean of the 2090–2100 annual SST) to calculate anticipated increase in temperature by 2100 (Supplementary Table 5). This methodology was used so that the warming estimates would be less dependent on year-to-year climate variability events.

Predicting changes in DO due to warming

We calculated changes in DO concentrations as a result of the physical and biological effects of temperature rise on DO solubility and biological oxygen demand (that is, total respiration rates), respectively, based on measured DO at each reef site and the projected CMIP6 temperature rise for each location. A simple box model was also used to validate the methodology and calculations used to approximate changes in DO solubility and biological oxygen demand (Supplementary Methods and Extended Data Fig. 5).

Calculating the impact of warming on solubility

Changes in DO solubility were calculated for each site under each climate projection ($DO_{sol\_SSP1\text{-}2.6}$, $DO_{sol\_SSP2\text{-}4.5}$, $DO_{sol\_SSP3\text{-}7.0}$, $DO_{sol\_SSP5\text{-}8.5}$) and a 6 °C heatwave scenario ($DO_{sol\_heatwave}$) using equations (4) and (5)[65] assuming only changes in temperature:

$$T_s = \ln\left(\frac{(298.15 - t)}{(273.15 + t)}\right) \tag{4}$$

$$\begin{aligned}\ln(DO_{sol}) = {} & A_0 + A_1 T_s + A_2 T_s^2 + A_3 T_s^3 + A_4 T_s^4 + A_5 T_s^5 \\ & + S\left(B_0 + B_1 T_s + B_2 T_s^2 + B_3 T_s^3\right) + C_0 S^2\end{aligned} \tag{5}$$

where t is temperature (°C), T_s is the scaled temperature, DO_{sol} is the solubility (μmol O_2 kg^{-1}), A_0 is 5.80818, A_1 is 3.20684, A_2 is 4.11890, A_3 is 4.93845, A_4 is 1.01567, A_5 is 1.41575, B_0 is -7.01211×10^{-03}, B_1 is -7.25958×10^{-03}, B_2 is -7.93334×10^{-03}, B_3 is -5.54491×10^{-03}, C_0 is -1.32412×10^{-07} and S is salinity (psu) (coefficients provided in ref. [65] in units of μmol kg^{-1}).

Changes in DO concentration as a result of changes in solubility (ΔDO_{sol}) due to warming from the present day were then calculated for each site and projection:

$$\Delta DO_{sol} = DO_{sol\_present} - DO_{sol\_proj} \tag{6}$$

where $DO_{sol\_present}$ is the solubility of DO under present-day measured temperature and salinity conditions (μmol O_2 kg^{-1}) and DO_{sol_proj} is the solubility of DO for a given temperature rise projection or scenario, calculated from equations (4) and (5) (μmol O_2 kg^{-1}).

Calculating the impact of warming on respiration

The respiration signal of each reef from the present day was approximated from the difference between the mean DO ($\overline{DO}$, μmol O_2 kg^{-1}) across the entire deployment and the mean daily minimum DO concentration ($\overline{DO}_{min}$, μmol O_2 kg^{-1}), according to equation (7):

$$DO_{offset} = \overline{DO} - \overline{DO}_{min} \tag{7}$$

Thus, DO_{offset} (μmol O_2 kg^{-1}) reflects the observed changes in DO owing to the net effect of nighttime respiration, air–sea gas exchange and physical transport processes, assuming that, on average, the daily mean DO at each location is close to 100% saturation. However, since air–sea gas exchange is quantitatively small relative to respiration rates on coral reefs and the flow is from air to sea at night, gas exchange was assumed to be negligible although it leads to a slight underestimation of the respiration signal. Similarly, day-to-day changes in water transport, current speed, trajectory and residence time could also influence the observed DO loss, but on average, each site is characterized by a set of baseline conditions constrained by the tidal cycle, depth, geomorphology, wind and swell conditions, which favours the application of DO_{offset} as an approximation of the respiration signal at each location. The daily statistics of DO_{offset} were calculated excluding the first and last days of the deployment in order to exclude partial days (less than full 24 h periods) from the mean.

To assess the biological impacts of each temperature rise scenario on biological oxygen demand, the change in respiration rate was calculated using a Q_{10} relationship according to equations (8) and (9) for each site and temperature scenario:

$$T_{rise} = T_2 - T_1 \tag{8}$$

$$R_2 = R_1 Q_{10}^{\left(\frac{T_{rise}}{10}\right)} \tag{9}$$

where T_{rise} is the difference between observed present-day T_1 and projected T_2, R_2 is the respiration rate under increased temperature T_2, R_1 is the respiration rate at present temperature (T_1) and Q_{10} is the unitless metabolic rate quotient[66,67]. In the present study, we assumed a Q_{10} of 2 (that is, metabolic rate, in this case respiration, doubles for every temperature increase of 10 °C), based on the literature for coral metabolism[68–72]. However, because absolute respiration rates were unknown (that is, R_1), the reduction in DO concentrations due to increased respiration under different warming scenarios was calculated based on the ratio of R_2 and R_1 and the estimated respiration signal, DO_{offset}, according to equations (10) and (11) (Extended Data Fig. 4):

$$DO_{offset_{Q_{10}}} = DO_{offset}\left(\frac{R_2}{R_1}\right) \tag{10}$$

$$\Delta DO_{Q_{10}} = DO_{offset_{Q_{10}}} - DO_{offset} \tag{11}$$

where $DO_{offset_{Q_{10}}}$ (μmol O_2 kg^{-1}) is the expected change in DO_{offset} (change in DO due to respiration at present) as a result of increased respiration and $\Delta DO_{Q_{10}}$ is the decrease in DO concentration, accounting for present-day respiration rates.

Combined impacts of warming on solubility and respiration

Combining the physical (changes in solubility) and biological (changes in respiration rate) effects of temperature rise, expected net reduction in DO concentration for each reef site and under each scenario was calculated using equations (12) and (13) (Extended Data Fig. 4):

$$\Delta DO = \Delta DO_{Q_{10}} + \Delta DO_{sol} \quad (12)$$

$$DO_{proj} = DO - \Delta DO \quad (13)$$

where ΔDO ($\mu mol\ O_2\ kg^{-1}$) is the total combined decrease in DO concentration, DO_{proj} is the projected DO concentration ($\mu mol\ O_2\ kg^{-1}$) for each site under each warming scenario, and DO is the present-day measured DO concentration at each site ($\mu mol\ O_2\ kg^{-1}$).

Reporting summary

Further information on research design is available in the Nature Portfolio Reporting Summary linked to this article.

Data availability

All data included in this study (for all figures and statistics[56]) are freely available on Dryad (https://doi.org/10.5061/dryad.41ns1rnj7). Data may be used if cited appropriately.

Code availability

All code files written and used for analyses in this study[57] are freely available on GitHub (https://github.com/apezner/GlobalReefOxygen). Code may be used if cited appropriately.

References

46. Yates, K. K., Moore, C. S. & Smiley, N. A. *Time Series of Autonomous Carbonate System Parameter Measurements from Crocker Reef, Florida, USA* (US Geological Survey, 2019); https://doi.org/10.5066/P90NCI8T
47. Kekuewa, S. A. H. et al. Temporal and spatial variabilities of chemical and physical parameters on the Heron Island coral reef platform. *Aquat. Geochem.* **27**, 241–268 (2021).
48. Pedersen, K. A. *Spatiotemporal Variability in Seawater Carbonate Chemistry at Two Contrasting Reef Locations in Bocas del Toro, Panama*. MSc thesis, Univ. California (2019).
49. Page, H. N. et al. Spatiotemporal variability in seawater carbon chemistry for a coral reef flat in Kāne'ohe Bay, Hawai'i. *Limnol. Oceanogr.* **64**, 913–934 (2018).
50. Pezner, A. K. et al. Lateral, vertical, and temporal variability of seawater carbonate chemistry at Hog Reef, Bermuda. *Front. Mar. Sci.* **8**, 1–18 (2021).
51. Ecosystem Sciences Division *National Coral Reef Monitoring Program: Diel Seawater Carbonate Chemistry Observations from a Suite of Instrumentation Deployed at Coral Reef Sites at Tutuila Island, American Samoa from June 23 to July 17, 2018* NCEI Accession 0240606 (Pacific Islands Fisheries Science Center, 2021).
52. Ecosystem Sciences Division *National Coral Reef Monitoring Program: Diel Seawater Carbonate Chemistry Observations from a Suite of Instrumentation Deployed at Coral Reef Sites at Baker Island, Jarvis Island, and Palmyra Atoll in the Pacific Remote Islands Marine National Monument Between 2018-06-12 and 2018-08-07* NCEI Accession 0240686 (Pacific Islands Fisheries Science Center, 2021).
53. Rintoul, M. S. et al. The effects of light intensity and flow speed on biogeochemical variability within a fringing coral reef in Onna-son, Okinawa, Japan. *J. Geophys. Res. Oceans* **127**, e2021JC018369 (2022).
54. Kelley, D. & Richards, C. gsw: Gibbs sea water functions. R package version 1.0-5 https://CRAN.R-project.org/package=gsw (2017).
55. RStudio Team RStudio: Integrated Development for R (RStudio, 2020).
56. Pezner, A. K. et al. Data for: Increasing hypoxia on global coral reefs under ocean warming. *Dryad* https://doi.org/10.5061/dryad.41ns1rnj7 (2023).
57. Pezner, A. K. et al. Global reef oxygen. *GitHub* https://github.com/apezner/GlobalReefOxygen (2023).
58. Kennedy, E. V. et al. Reef cover, a coral reef classification for global habitat mapping from remote sensing. *Sci. Data* **8**, 196 (2021).
59. Dowle, M. & Srinivasan, A. data.table: extension of 'data.frame'. R package version 1.13.6 https://CRAN.R-project.org/package=data.table (2020).
60. Rosenberg, R. in *Fjord Oceanography: Effects of Oxygen Deficiency on Benthic Macrofauna in Fjord oceanography*, H. J. Freeland, D. M. Farmer, and C. D. Levings (eds), 499–514 (Plenum Press, 1980).
61. Hofmann, A. F., Peltzer, E. T., Walz, P. M. & Brewer, P. G. Hypoxia by degrees: establishing definitions for a changing ocean. *Deep Sea Res. I* **58**, 1212–1226 (2011).
62. Klein, S. G., Steckbauer, A. & Duarte, C. M. Defining CO_2 and O_2 syndromes of marine biomes in the Anthropocene. *Glob. Change Biol.* **26**, 355–363 (2020).
63. Danabasoglu, G. *NCAR CESM2-WACCM Model Output Prepared for CMIP6 CMIP* (Earth System Grid Federation, 2019); https://doi.org/10.22033/ESGF/CMIP6.10028
64. Danabasoglu, G. *NCAR CESM2-WACCM Model Output Prepared for CMIP6 ScenarioMIP* (Earth System Grid Federation, 2019); https://doi.org/10.22033/ESGF/CMIP6.10101
65. Garcia, H. E. & Gordon, L. I. Oxygen solubility in seawater: better fitting equations. *Limnol. Oceanogr.* **37**, 1307–1312 (1992).
66. Hochachka, P. W. & Somero, G. N. *Biochemical Adaptations* (Oxford Univ. Press, 2002).
67. Brown, J. H., Gillooly, J. F., Allen, A. P., Savage, V. M. & West, G. B. Toward a metabolic theory of ecology. *Ecology* **85**, 1771–1789 (2004).
68. Clausen, C. D. & Roth, A. A. Effect of temperature and temperature adaptation on calcification rate in the hermatypic coral *Pocillopora damicornis*. *Mar. Biol.* **33**, 93–100 (1975).
69. Howe, S. A. & Marshall, A. T. Thermal compensation of metabolism in the temperate coral, *Plesiastrea versipora* (Lamarck, 1816). *J. Exp. Mar. Biol. Ecol.* **259**, 231–248 (2001).
70. Edmunds, P., Gates, R. & Gleason, D. The biology of larvae from the reef coral *Porites astreoides*, and their response to temperature disturbances. *Mar. Biol.* **139**, 981–989 (2001).
71. Edmunds, P. J. Effect of elevated temperature on aerobic respiration of coral recruits. *Mar. Biol.* **146**, 655–663 (2005).
72. Edmunds, P. J. Differential effects of high temperature on the respiration of juvenile Caribbean corals. *Bull. Mar. Sci.* **83**, 453–464 (2008).

Acknowledgments

We thank K. Inoha, R.-W. Syu and all field station administrators and field assistants who were essential in collecting these datasets. Any use of trade, firm or product names is for descriptive purposes only and does not imply endorsement by the US Government. Funding was provided by the National Science Foundation: OCE-1255042 (A.J.A.), OCE-1829778 (A.J.A.), OCE-1538495 (D.I.K. and M.T.), OCE-1459255 (M.D.D) and OPP-1951294 (M.D.D); Belmont Forum/NSF ICER 2029205 (A.J.A.); UCSD Marine Sciences grant no. A105437 (A.J.A.); the National Science Foundation Graduate Research Fellowship DGE-2038238 (A.K.P.); a Philanthropic Educational Organization International Scholar Award (A.K.P.); the NOAA Coral Reef Conservation Program and NOAA Ocean Acidification Program, through the NOAA National Coral Reef Monitoring Program (H.C.B.); the US Geological Survey Coastal and Marine Hazards and Resources Program-funded data collection at Crocker Reef, Florida, USA (K.K.Y.[46]); internal funding from the Okinawa Institute of Science and Technology (S.M.); and the Ministry of Science and Technology of Taiwan grant no. 107-2611-M-019-001-MY3 (W.-C.C.). Funding for the long-term monitoring programme on Palmyra Atoll was provided to Smith Lab (J.E.S.) from the Bohn Family Foundation and the Bill and Kathy Scripps Family Foundation.

Author contributions

A.K.P., T.A.C. and A.J.A. conceptualized the paper and methodology, with contributions from M.S.R. to methodology. A.K.P. performed the formal analysis and visualization, under supervision of T.A.C. and A.J.A. A.K.P. and A.J.A. wrote the original draft of the paper. All authors (A.K.P., T.A.C., H.C.B., W.-C.C., H.-C.C., S.M.C., T.C., M.D.G, S.A.H.K., D.I.K., Y.-B.L., T.R.M., S.M., H.N.P., M.S.R., J.E.S., K.S., Y.T., M.T., Y.W., K.K.Y. and A.J.A.) contributed to investigation as well as review and editing of the paper.

Competing interests

The authors declare no competing interests.

Additional information

Extended data is available for this paper at https://doi.org/10.1038/s41558-023-01619-2.

Supplementary information The online version contains supplementary material available at https://doi.org/10.1038/s41558-023-01619-2.

Correspondence and requests for materials should be addressed to Ariel K. Pezner.

Peer review information *Nature Climate Change* thanks Rachel Alderdice, Christopher Cornwall and the other, anonymous, reviewer(s) for their contribution to the peer review of this work.

Reprints and permissions information is available at www.nature.com/reprints.

https://doi.org/10.1038/s41558-023-01619-2

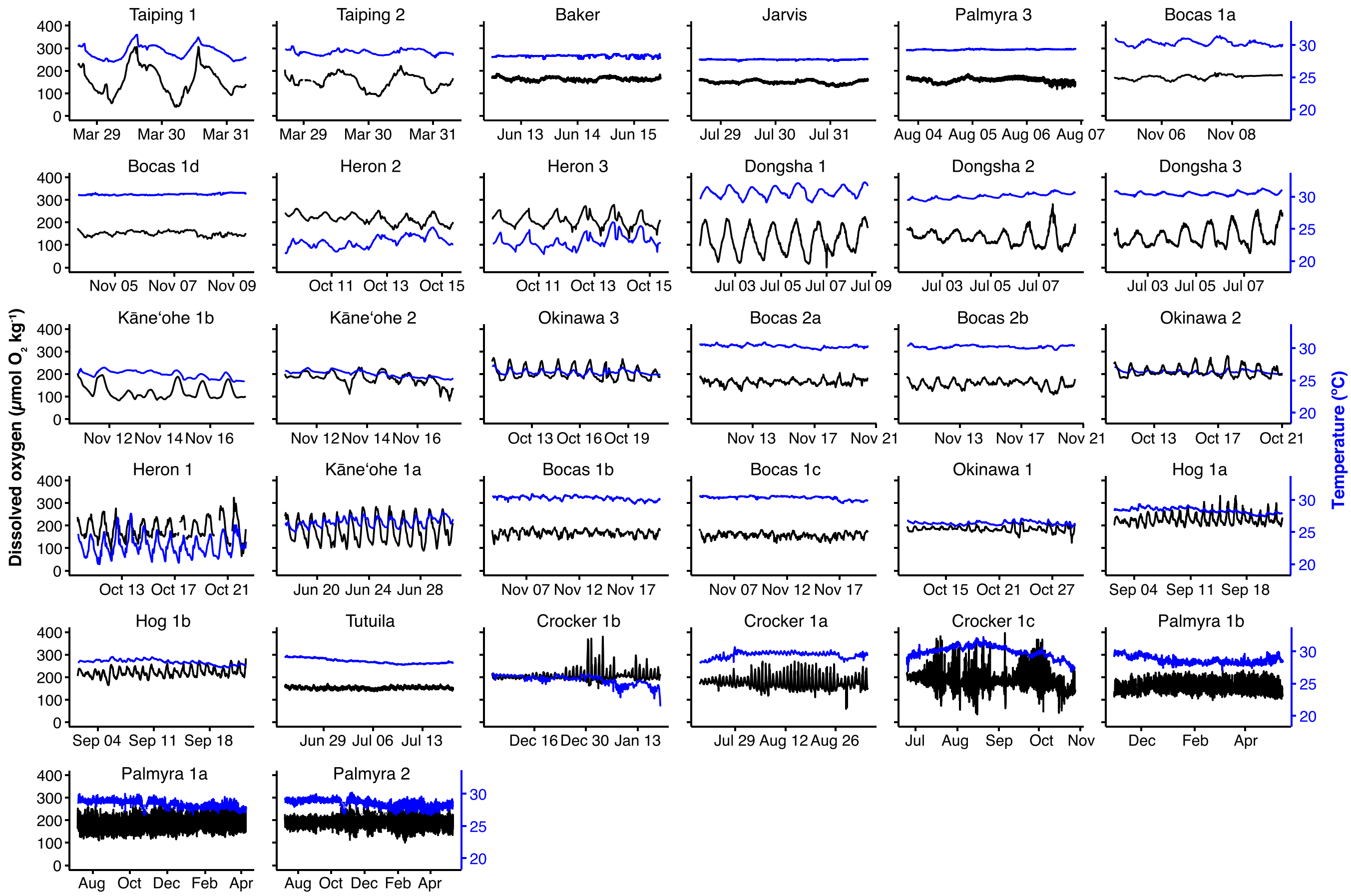

Extended Data Fig. 1 | Dissolved oxygen and temperature time series for global coral reef sites. Dissolved oxygen (μmol O_2 kg^{-1}; black, left y-axis) and temperature (°C; blue, right y-axis) as a function of time in order of sites with increasing deployment length, ranging from 3 to 309 days (Supplementary Table 1). For each location, different instrument deployment sites are represented by numbers (for example, Dongsha 1 and Dongsha 2), or a combination of letters and numbers where letters represent either different depths at the same site (for example, Bocas 1a and 1b) or different deployments at the same site over time (for example, Crocker 1a, 1b, and 1c) (see Supplementary Table 1 for specific site information).

https://doi.org/10.1038/s41558-023-01619-2

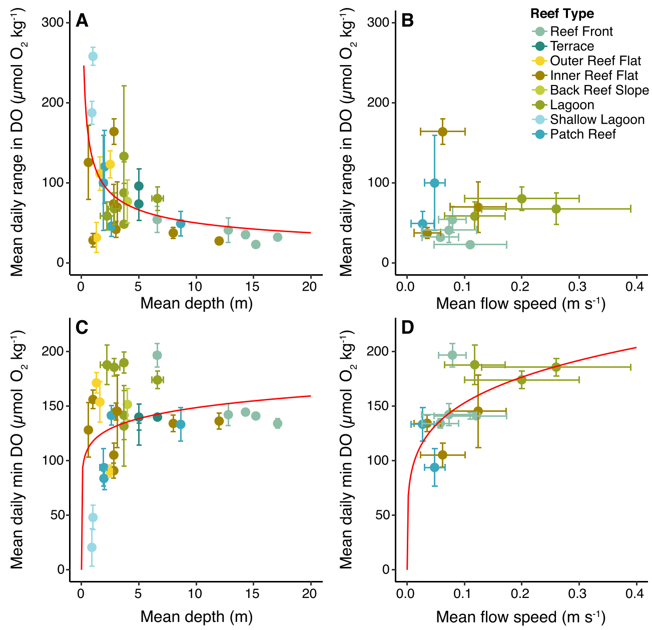

Extended Data Fig. 2 | Nonlinear regressions between dissolved oxygen metrics, depth, and flow speed categorized by reef type. (**a**) Dissolved oxygen (DO) variability (mean daily range in DO; μmol O_2 kg^{-1}; ±1 standard deviation (s.d.)) as a function of mean depth (m; ±1 s.d.) and (**b**) mean flow speed (m s^{-1}; ±1 s.d.) at global coral reef sites categorized by reef type (colors; Supplementary Table 1). (**c**) Mean daily minimum DO (μmol O_2 kg^{-1}; ±1 s.d.) as a function of mean depth (m; ±1 s.d.) and (**d**) mean flow speed (m s^{-1}; ±1 s.d.). For DO metrics, error bars represent ±1 s.d. (n varies by site, see Supplementary Table 2). Measurements of flow speed and depth were only made at a subset of locations (n varied by site, see Supplementary Table 3). Error bars also represent ±1 s.d. for the sites where these data were recorded. For sites where no current meter was deployed, recorded deployment depth was used instead of a calculated mean depth (no error bars plotted). Regression lines were plotted using power model regression statistics reported in Supplementary Table 4. No regression line is plotted in **B** due to poor fit.

https://doi.org/10.1038/s41558-023-01619-2

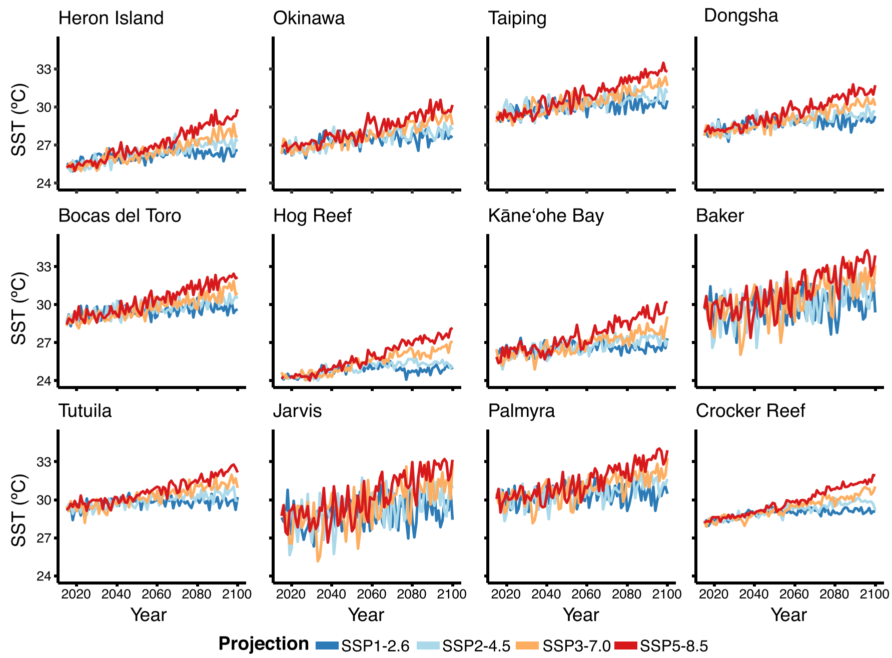

Extended Data Fig. 3 | Sea surface temperature predictions for global coral reef locations. Mean monthly Coupled Model Intercomparison Project 6 (CMIP6) ensemble member Community Earth System Model 2 Whole Atmosphere Community Climate Model (CESM2-WACCM)[63,64] sea surface temperature (SST) projections at global coral reef sites for the Shared Socioeconomic Pathways (SSPs) SSP1-2.6, SSP2-4.5, SSP3-7.0, and SSP5-8.5 scenarios (blue to red) between 2015 and 2100.

 https://doi.org/10.1038/s41558-023-01619-2

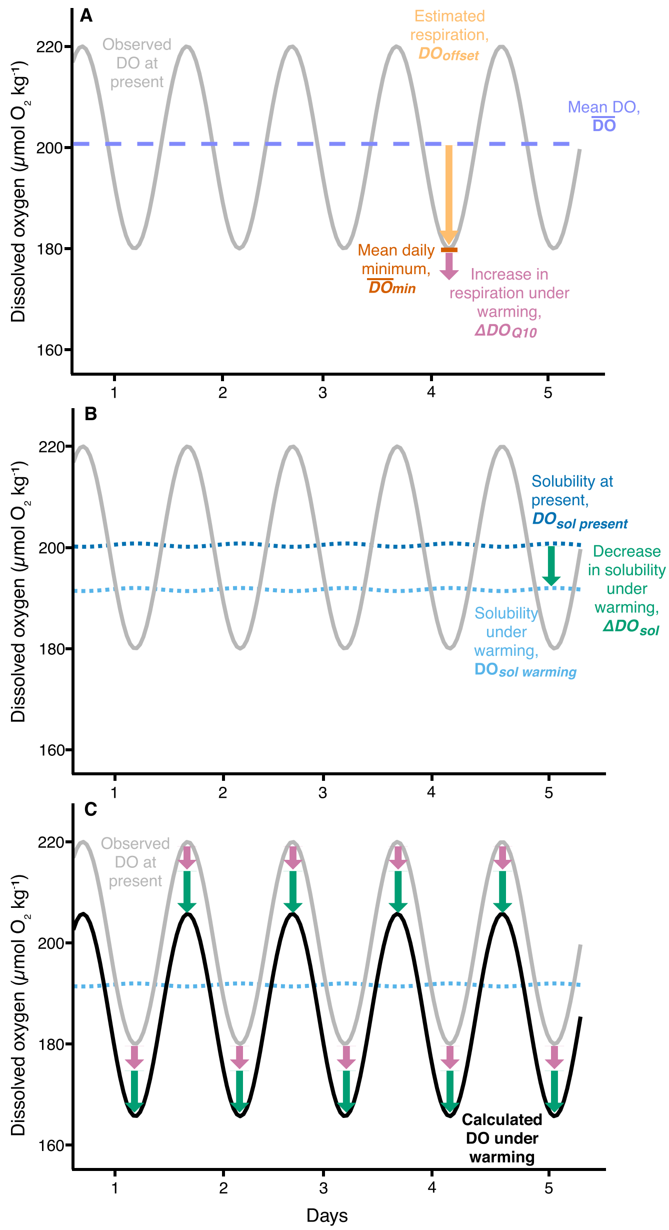

Extended Data Fig. 4 | Conceptual diagram of calculation approach used to estimate changes in coral reef dissolved oxygen under warming (Equations 6–13). (**a**) Present-day dissolved oxygen (DO; µmol O_2 kg^{-1}; solid grey line), mean DO value across time series (purple dashed line; assumed to be close to equilibrium), approximation of drawdown of DO by respiration at night (DO_{offset}; yellow arrow) expressed as the difference between mean DO and mean daily minimum (DO_{min}; orange), and the projected increase in respiration under 3 °C warming using a Q_{10} relationship (ΔDO_{Q10}; pink arrow). (**b**) Present-day DO (solid grey line), present-day DO solubility (dashed dark blue line; $DO_{sol\ present}$), DO solubility under 3 °C warming (dashed light blue line), and the calculated decrease in solubility under 3 °C warming (ΔDO_{sol}; green arrow). (**c**) Present-day DO (solid grey line) and new calculated DO under 3 °C warming (black solid line) due to increased respiration and decreased solubility (pink and green arrows, respectively).

 https://doi.org/10.1038/s41558-023-01619-2

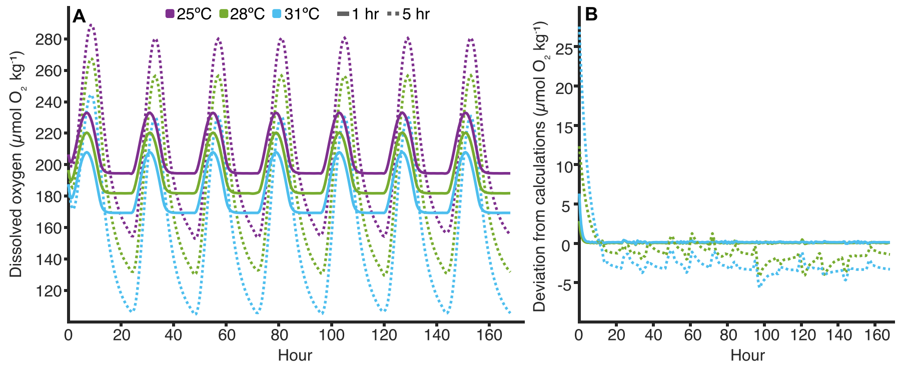

Extended Data Fig. 5 | Box model simulations and validation of calculation approach to estimate dissolved oxygen changes as a result of warming. (**a**) Modeled variations in seawater dissolved oxygen (DO; µmol O_2 kg^{-1}) in a hypothetical coral reef system over 7 days under three temperature scenarios (25 °C, 28 °C, and 31 °C; purple, green, blue, respectively) and two residence times (1 hour and 5 hours; solid and dotted lines, respectively). The model is described in detail in the Supplementary Information Extended Methods. (**b**) Comparison between the box model-calculated changes in DO due to warming and the calculation approach employed for the global coral reef dataset (Extended Data Fig. 4; Equations 6–13) represented as the deviation of model DO estimates from calculation DO estimates (µmol O_2 kg^{-1}). Comparisons were made for two warming scenarios relative to the base scenario of 25 °C (+3 °C and +6 °C; blue and green, respectively) and two residence times (1 hour and 5 hours; solid and dotted, respectively) over 7 days.

https://doi.org/10.1038/s41558-023-01619-2

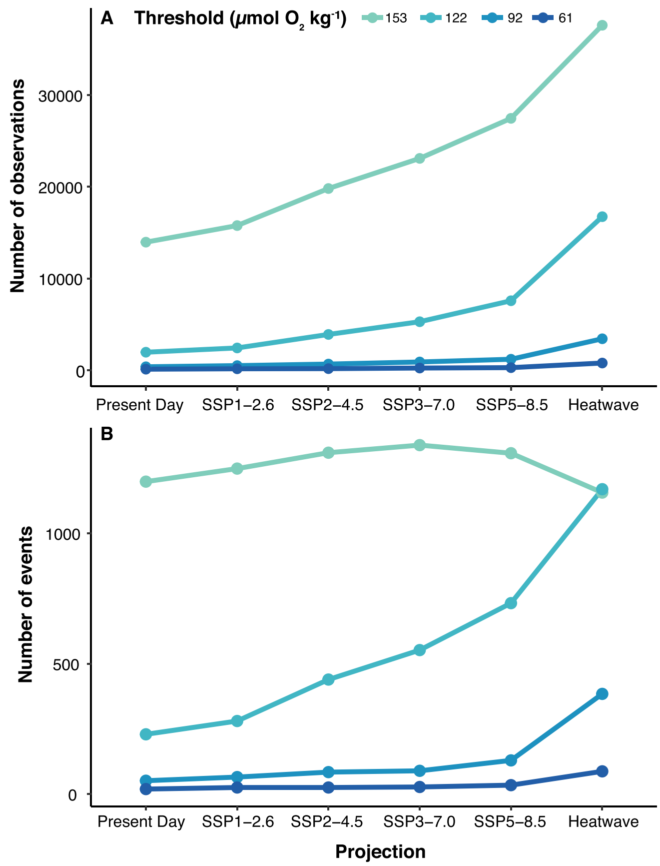

Extended Data Fig. 6 | Total number of hypoxic observations and events for global coral reef sites under different warming scenarios and hypoxia thresholds. (**a**) Total number of observations and (**b**) total number of hypoxic events below different hypoxia thresholds: 153 μmol O_2 kg^{-1}, 122 μmol O_2 kg^{-1}, 92 μmol O_2 kg^{-1}, and 61 μmol O_2 kg^{-1} (weak, mild, moderate, and severe; light blue to dark blue) for different warming scenarios including 4 Shared Socioeconomic Pathways (SSPs) and a heatwave event across global coral reef sites.

https://doi.org/10.1038/s41558-023-01619-2

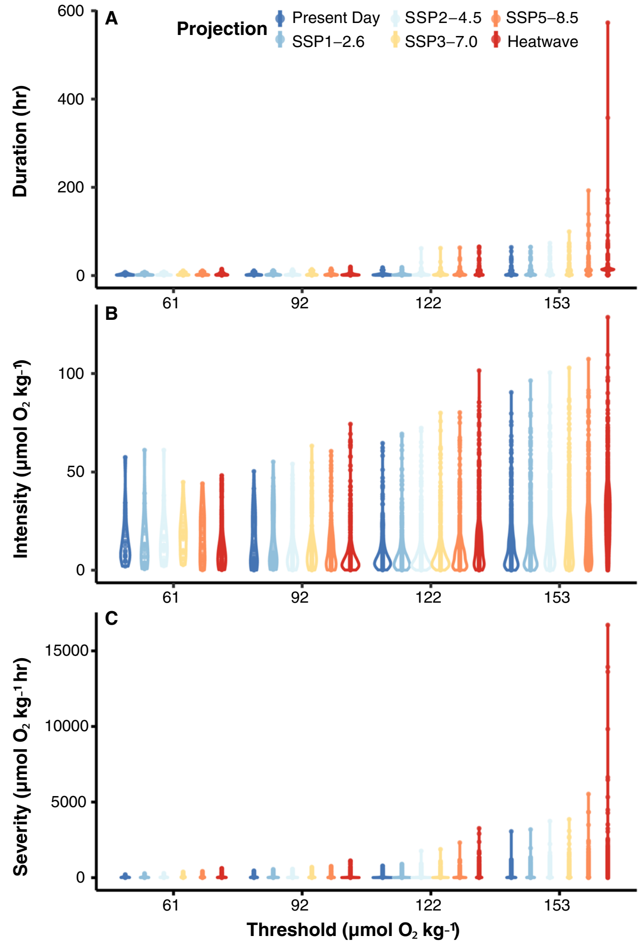

Extended Data Fig. 7 | Changes in the duration, intensity, and severity of hypoxic events under warming for global coral reef sites. Distributions of the (**a**) duration (hours), (**b**) intensity (µmol O_2 kg^{-1}), and (**c**) severity (µmol O_2 kg^{-1} hr) of hypoxic events below different oxygen thresholds (≤153 µmol O_2 kg^{-1}, ≤122 µmol O_2 kg^{-1}, ≤92 µmol O_2 kg^{-1}, or ≤61 µmol O_2 kg^{-1}) under present-day conditions and 5 different warming projections (including 4 Shared Socioeconomic Pathways (SSPs); blue to red) across global coral reef sites.

https://doi.org/10.1038/s41558-023-01619-2

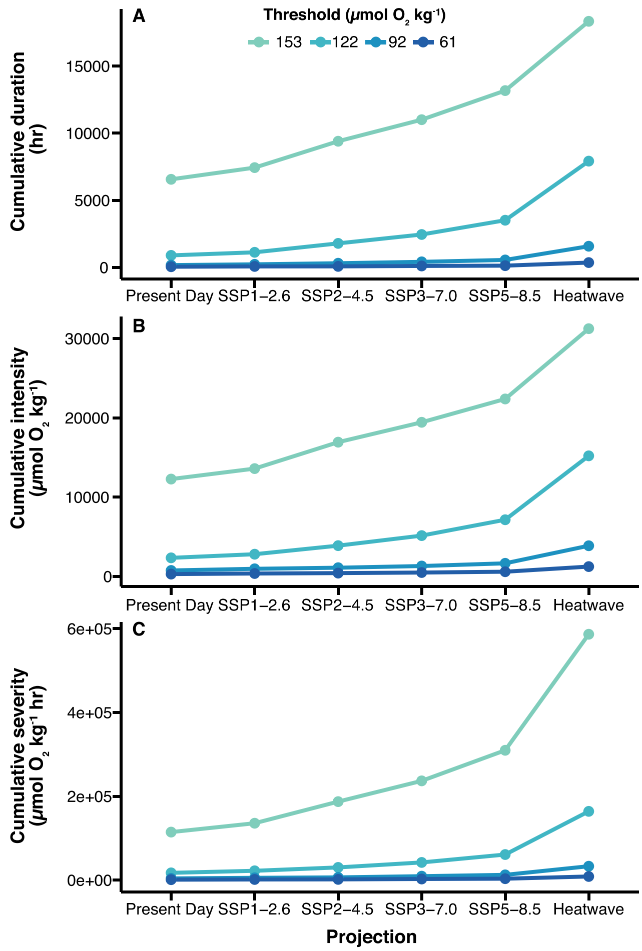

Extended Data Fig. 8 | Changes in the cumulative duration, intensity, and severity of hypoxic events under warming for global coral reef sites. (**a**) Cumulative duration (hours), (**b**) cumulative intensity (μmol O_2 kg^{-1}), and (**c**) cumulative severity (μmol O_2 kg^{-1} hr) of hypoxic events below different oxygen thresholds (≤153 μmol O_2 kg^{-1}, ≤122 μmol O_2 kg^{-1}, ≤92 μmol O_2 kg^{-1}, or ≤61 μmol O_2 kg^{-1}; shades of blue) for different warming scenarios including 4 Shared Socioeconomic Pathways (SSPs) and a heatwave event across global coral reef sites.

nature research

Corresponding author(s): Ariel K. Pezner

Last updated by author(s): January 20, 2023

Reporting Summary

Nature Research wishes to improve the reproducibility of the work that we publish. This form provides structure for consistency and transparency in reporting. For further information on Nature Research policies, see our Editorial Policies and the Editorial Policy Checklist.

Statistics

For all statistical analyses, confirm that the following items are present in the figure legend, table legend, main text, or Methods section.

n/a	Confirmed	
☐	☒	The exact sample size (n) for each experimental group/condition, given as a discrete number and unit of measurement
☐	☒	A statement on whether measurements were taken from distinct samples or whether the same sample was measured repeatedly
☒	☐	The statistical test(s) used AND whether they are one- or two-sided *Only common tests should be described solely by name; describe more complex techniques in the Methods section.*
☒	☐	A description of all covariates tested
☒	☐	A description of any assumptions or corrections, such as tests of normality and adjustment for multiple comparisons
☐	☒	A full description of the statistical parameters including central tendency (e.g. means) or other basic estimates (e.g. regression coefficient) AND variation (e.g. standard deviation) or associated estimates of uncertainty (e.g. confidence intervals)
☒	☐	For null hypothesis testing, the test statistic (e.g. F, t, r) with confidence intervals, effect sizes, degrees of freedom and P value noted *Give P values as exact values whenever suitable.*
☒	☐	For Bayesian analysis, information on the choice of priors and Markov chain Monte Carlo settings
☒	☐	For hierarchical and complex designs, identification of the appropriate level for tests and full reporting of outcomes
☒	☐	Estimates of effect sizes (e.g. Cohen's d, Pearson's r), indicating how they were calculated

Our web collection on statistics for biologists contains articles on many of the points above.

Software and code

Policy information about availability of computer code

Data collection	All autonomous sensor data was collected in the field in situ. Temperature projection data were downloaded from the CMIP6 data repository (https://esgf-node.llnl.gov/search/cmip6/). No software was used.
Data analysis	All code for data analysis was written using RStudio (version 3.6.2) and the simple box model was constructed using MATLAB (version R2019a). All code is available in a public GitHub repository (https://github.com/apezner/GlobalReefOxygen) and all data is available for free at Dryad (https://doi.org/10.5061/dryad.41ns1rnj7). Specific R and MATLAB functions used are denoted in the text and cited accordingly.

For manuscripts utilizing custom algorithms or software that are central to the research but not yet described in published literature, software must be made available to editors and reviewers. We strongly encourage code deposition in a community repository (e.g. GitHub). See the Nature Research guidelines for submitting code & software for further information.

Data

Policy information about availability of data

All manuscripts must include a data availability statement. This statement should provide the following information, where applicable:

- Accession codes, unique identifiers, or web links for publicly available datasets
- A list of figures that have associated raw data
- A description of any restrictions on data availability

All data included in this study (for all figures and statistics) are freely available on Dryad (https://doi.org/10.5061/dryad.41ns1rnj7).

Field-specific reporting

Please select the one below that is the best fit for your research. If you are not sure, read the appropriate sections before making your selection.

☐ Life sciences ☐ Behavioural & social sciences ☒ Ecological, evolutionary & environmental sciences

For a reference copy of the document with all sections, see nature.com/documents/nr-reporting-summary-flat.pdf

Ecological, evolutionary & environmental sciences study design

All studies must disclose on these points even when the disclosure is negative.

Study description	This study uses autonomous sensor data (dissolved oxygen concentration and saturation, temperature, and salinity) from 32 different deployments in coral reef ecosystems at 12 locations to explore dissolved oxygen concentrations across a global coral reef dataset. This study also employs modeled temperature projection data from the Coupled Model Intercomparison Project 6 (CMIP6) ensemble member Community Earth System Model Whole Atmosphere Community Climate Model (CESM2-WACCM) for each of the 12 locations to project how warming will impact hypoxia duration, intensity, and severity on reefs by the end of the century.
Research sample	This study synthesized dissolved oxygen, temperature, and salinity datasets collected in tropical coral reef habitats around the world. These data were collated to provide the broad spatial and temporal coverage needed to characterize dissolved oxygen trends on global tropical coral reefs. These data represent some of few available oxygen datasets from these environments. Of the 32 datasets, 24 datasets collected by co-authors have been previously published and/or are publicly available (Kekuewa et al., 2021; Pedersen, 2019; Page et al., 2018; Yates et al., 2019; Pezner et al., 2021; Ecosystem Sciences Division, 2021a,b; Rintoul et al., 2022), while 8 datasets are being presented for the first time in the present study and are freely available in an online repository (https://doi.org/10.5061/dryad.41ns1rnj7). Temperature projection data from the CMIP6 CESM2-WACCM is publicly available (https://esgf-node.llnl.gov/search/cmip6/) and was selected to provide location-specific projections of warming for each of the 12 locations.
Sampling strategy	Sample sizes of the autonomous sensor data were determined by the researchers who collected the datasets and were based on sensor performance, field time, ship time, weather, and original study objectives.
Data collection	Autonomous sensor data were recorded by the specified instruments (e.g., SeapHOx, Sea-Bird, MiniDOT, Idronaut, and Aanderaa sensors) by each research team in the field and converted to compatible data formats after instrument recovery. Temperature projection data from the CMIP6 CESM2-WACCM were downloaded from the CMIP6 data repository (https://esgf-node.llnl.gov/search/cmip6/).
Timing and spatial scale	Deployment dates varied for each of the 32 datasets, ranging from several days to nearly one year, and were all collected between 2015 and 2019. Sensors recorded data at frequencies ranging from every 1 minute to every 1 hour. Prior to analysis, all datasets were either sub-sampled or interpolated to have 30-minute sampling frequencies for consistency. Data from individual deployments represent relatively small spatial scales (a few meters), but altogether the observational data presented include reef sites between 23 ºS and 32 ºN in the East and South China Sea; North Atlantic; West, Central, and South Pacific; and Caribbean over several years.
Data exclusions	Data were assessed for quality and erroneous data points (defined as missing values or values that exceeded the measurement range of the instrument), which were flagged and excluded from any subsequent analyses. Deployment data were restricted to measurements in seawater based on salinity values to exclude extraneous data points collected during instrument transport, initial deployment, or recovery (exposure to air).
Reproducibility	Latitude, longitude, depth, and deployment dates are provided for all sensor deployments. Calculations and statistics are reproducible using the provided data and code files. The methodology for calculating oxygen projections under warming based on the sensor data and CMIP6 temperature projections was also confirmed with a simple box model included in the code provided (https://github.com/apezner/GlobalReefOxygen).
Randomization	Deployment sites of autonomous sensors were chosen haphazardly based on accessibility and safety considerations.
Blinding	No experiments were conducted for this study, therefore blinding was not required.

Did the study involve field work? ☒ Yes ☐ No

Field work, collection and transport

Field conditions	Field conditions varied by location and site, but generally involved boat-, SCUBA-, and/or snorkel-based expeditions in shallow coral reef environments.
Location	Data were collected from Bocas del Toro, Panama; Crocker Reef, Florida, USA; Hog Reef, Bermuda; Heron Island, Australia; Kāne'ohe Bay, Hawai'i, USA; Dongsha Atoll, Taiwan; Okinawa, Japan; Baker Island; Jarvis Island; Palmyra Atoll; Tutuila, American Samoa; and multiple sites within many of these locations.
Access & import/export	All deployments were performed in collaboration with local collaborators in compliance with local, national, and international laws. No samples were exported/imported for this study.

Disturbance	All possible efforts were made to reduce disturbance to reef habitats in the collection of these datasets (e.g. attaching sensors to cinderblocks or frames rather than live corals). No biological samples were collected or used in this study.

Reporting for specific materials, systems and methods

We require information from authors about some types of materials, experimental systems and methods used in many studies. Here, indicate whether each material, system or method listed is relevant to your study. If you are not sure if a list item applies to your research, read the appropriate section before selecting a response.

Materials & experimental systems

n/a	Involved in the study
☒	☐ Antibodies
☒	☐ Eukaryotic cell lines
☒	☐ Palaeontology and archaeology
☒	☐ Animals and other organisms
☒	☐ Human research participants
☒	☐ Clinical data
☒	☐ Dual use research of concern

Methods

n/a	Involved in the study
☒	☐ ChIP-seq
☒	☐ Flow cytometry
☒	☐ MRI-based neuroimaging